Supporting Information

A Low-Bandgap Dimeric Porphyrin Molecule for 10% Efficiency Solar Cells with Small Photon Energy Loss

Liangang Xiao,[a] Tianqi Lai,[a] Xiang Liu,[a] Feng Liu[c], Thomas P. Russell[d,e], Yi Liu[b,], Fei Huang[a,]*, Xiaobin Peng[a,]* and Yong Cao[a]*

[a] Institute of Polymer Optoelectronic Materials and Devices, State Key Laboratory of Luminescent Materials and Devices, South China University of Technology, 381 Wushan Road, Guangzhou 510640, China

Email: F.H: msfhuang@scut.edu.cn; X.P: chxbpeng@scut.edu.cn

[b] The Molecular Foundry, Lawrence Berkeley National Laboratory, Berkeley, California 94720, United States

E-mail: yliu@lbl.gov

[c] Department of Physics and Astronomy, and Collaborative Innovation Center of IFSA (CICIFSA), Shanghai Jiaotong University, Shanghai 200240, P. R. China

[d] Materials Sciences Division, Lawrence Berkeley National Lab, Berkeley, California 94720, United States

[e] Polymer Science and Engineering Department, University of Massachusetts, Amherst, Massachusetts 01003, United States

Experiment Details:

Materials: All reagents were purchased from commercial sources (Aldrich, Acros, Energy chemical or Suna Tech Inc.) and used as received. Tetrahydrofuran (THF) triethylamine (Et_3N) and toluene were dried over Na/benzophenoneketyl and freshly distilled prior to use.

Device Fabrication: The solution-processed BHJ solar cells were fabricated with a conventional device structure of Indium tin oxide (ITO)/PEDOT:PSS/ZnP2BT-RH:$PC_{71}BM$/PNDIT-F3N-Br/Al, and the fabrication details are as follows: ITO coated glass substrates were cleaned prior to device fabrication by sonication in acetone, detergent, distilled water, and isopropyl alcohol. After treated with an oxygen plasma for 4 min, 40 nm thick poly(styrene sulfonate)-doped poly(ethylene-dioxythiophene) (PEDOT:PSS) (Bayer Baytron 4083) layer was spin-casted on the ITO-coated glass substrates at 3000 rpm for 30 s, the substrates were subsequently dried at 150 ℃ for 10 min in air and then transferred to a N_2-glovebox. The active layers were prepared from ZnP2BT-RH:$PC_{71}BM$ in mixed solvent of chlorobenzene/pyridine (100:1 v/v) with an overall concentration of 30 mg/ml. The weight ratio of ZnP2BT-RH to $PC_{71}BM$ is varied from 1:1 to 1:2.5. For thermal annealing treatment, the active layer was annealed at different temperature for 5 mins. The optimal thermal annealing temperature is 135 ℃. For solvent vapor annealing treatment, the active layer was put in the petri dish containing 1 milliliter chloroform for different time. The optimal solvent vapor annealing time is 240 seconds. The

thicknesses of active layers measured by a profilometer were to be about 110nm. The ultra-thin conjugated poly[(9,9-bis(3'-((N,N-dimethyl)-N-ethylammonium)propyl)-2,7-fluorene)-alt-5,5'-bis(2,2'-thiophene)-2,6-naphthalene-1,4,5,8-tetracaboxylic-N,N'-di(2-ethylhexyl)imide]dibromide (PNDIT-F3N-Br) layer was deposited by spin casting from a 0.03% (w/v) solution in methanol (from 2000 rpm for 30 s). Finally, Al (~80 nm) was evaporated with a shadow mask as the top electrode. The effective area was measured to be 0.16 cm^2.

Measurements and Instruments: ^1H NMR spectra were recorded using a Bruker Ultrashield 500 Plus NMR spectrometer. High-resolution matrix-assisted laser desorption/ionization time-off light (MALDI-TOF) mass spectra were obtained with a Bruker Autoflex MALDITOF mass spectrometer. UV-vis spectra of dilute solutions of samples in dichloromethane (THF) were recorded at room temperature (ca. 25°C) using a Shimadzu UV-3600 spectrophotometer. Solid films for UV-vis spectroscopic analysis were obtained by spin-coating the solutions onto a quartz substrate. Cyclic voltammetry (CV) was carried out on a CHI660A electrochemical workstation with platinum electrodes at a rate of 50 mV s^{-1} against an Ag/AgCl reference electrode with nitrogen-staturated solution of 0.1 M tetrabutylammonium hexafluorophosphate (Bu_4NPF_6) in acetonitrile (CH_3CN).

PCEs were determined from J-V characteristics measured by a Keithley 2400 source-measurement unit under AM 1.5G spectrum from a solar simulator (Oriel model 91192). Masks made from laser beam cutting technology with a well-defined

area of 0.16 cm^2 were attached to define the effective area for accurate measurement. Solar simulator illumination intensity was determined using a monocrystal silicon reference cell (Hamamatsu S1133, with KG-5 visible color filter) calibrated by the National Renewable Energy Laboratory (NREL). The tapping mode atomic force microscopy (AFM) measurements of the blends' surface morphology were conducted on a NanoScope NS3A system (Digital Instrument). External quantum efficiency (EQE) values of the encapsulated devices were measured by using an integrated system (Enlitech, Taiwan, China) and a lock-in amplifier with a current preamplifier under short-circuit conditions. The devices were illuminated by monochromatic light from a 75 W xenon lamp. The light intensity was determined by using a calibrated silicon photodiode.

Grazing incidence X-ray diffraction (GIXD) characterization of the thin films was performed at beamline 7.3.3 Lawrence Berkeley National Lab. The scattering signal was recorded on a 2-D detector (Pilatus 1M) with a pixel size of 172 μm. The X-ray energy is 10 keV. The samples were ~15 mm long in the direction of the beam path, and the detector was located at a distance of 300 mm from the sample center (distance calibrated using a silver behenet standard). The incidence angle of 0.16° was chosen which gave the optimized signal-to-background ratio. Thin film samples were prepared on PEDOT:PSS covered silicon wafers to match the device conditions. The data was processed and analyzed using Nika software package. RSoXS was performed at beamline 11.0.1.2 Lawrence Berkeley National Lab. A 284.2 eV beamline energy at $PC_{61}BM$ k-edge was chosen to enhance the contrast. Thin films of

device thickness was flowed and transferred onto Si_3N_4 substrates, which were then mounted onto sample plate.

Capacitance-voltage characteristics: We measured the relative dielectric constants of all the materials with a device structure of ITO/PEDOT:PSS/small molecule or polymer films/Al. Capacitance-voltage (C-V) measurements were performed using a HP 4192A LCR meter by sweeping the voltage from -10V to +10V at room temperature, with ramping rate of 0.5 V/s and 30 mV of oscillator levels. Figure S7 shows corresponding dielectric constants of small molecule or polymer films with respect to frequency (10^3 to 5×10^5 H_Z). The dielectric constant was calculated from the following equation:

$$\varepsilon_r = \frac{Cd}{\varepsilon_0 A}$$

ε_r is the relative dielectric constant of the material, ε_0 is the dielectric constant of free space, d is the thickness of the active films, A is the capacitor area (0.16 cm^2), C is the capacitance of the device.

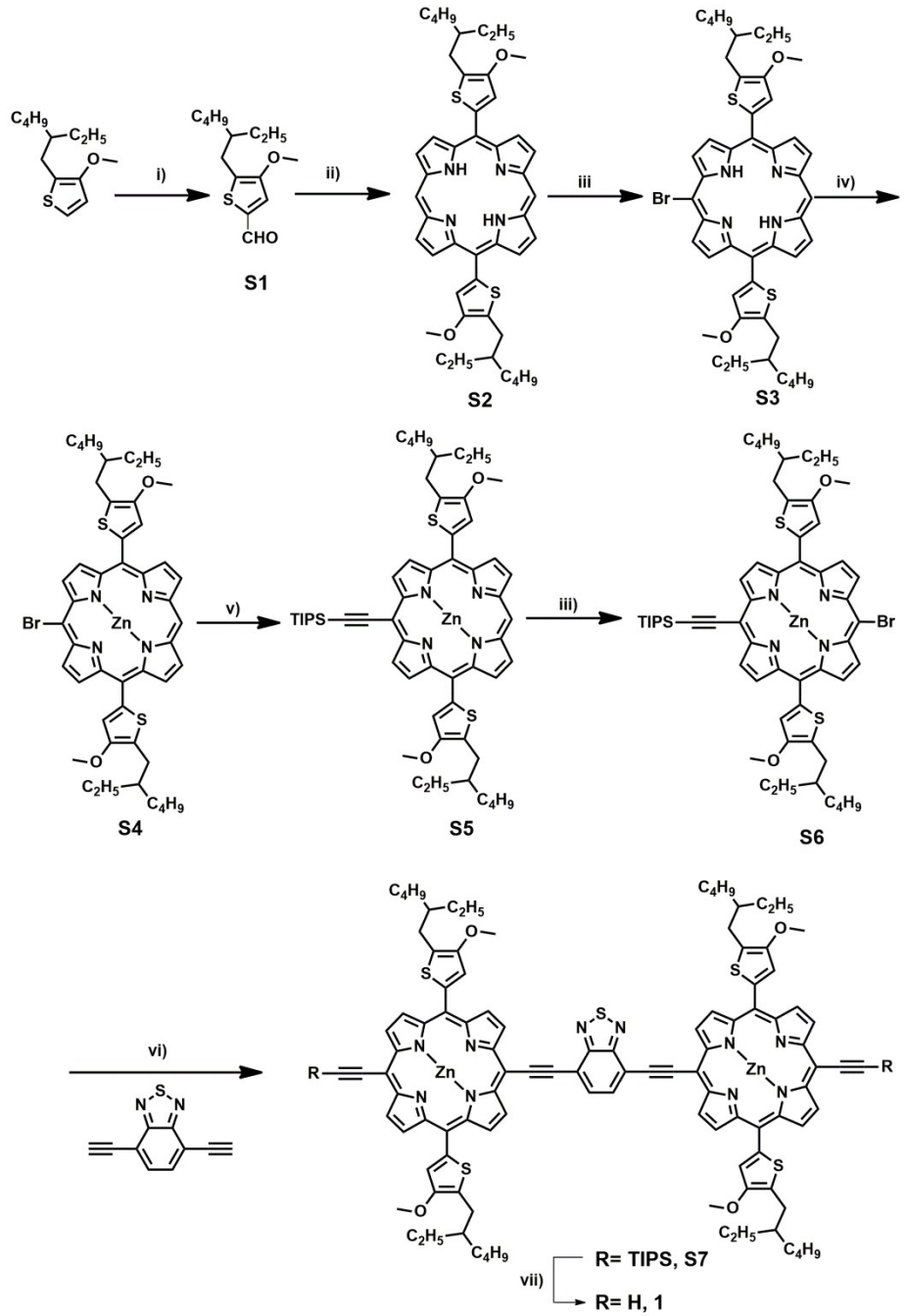

Scheme S1. Synthesis routes for porphyrin unit (1): (i)DMF, $POCl_3$; (ii)DCM, TFA, DDQ; (iii) NBS, $CHCl_3$; (iv) Zn(OAc)2, $CHCl_3$/MeOH; (v) TIPSA, $Pd(PPh_3)_2Cl_2$, CuI, THF/Et_3N; (vi) $Pd(PPh_3)_4$, CuI, THF/Et_3N; (vii)TBAF, THF.

We synthesized 2-(2-ethylhexyl)-3-methoxythiophene,[1] 5-bromo-10,20-bis[5-(2-ethylhexyl)-4-methoxythiophene-2-yl]-porphyrin(2)[2] and 4,7-Diethynyl-

benzo[*c*][1,2,5]thiadiazole[3] according to literature procedures.

5-(2-ethylhexyl)-4-methoxythiophene)-2-carbaldehyde (S1):

To a stirred solution of (2-(2-ethylhexyl)-3-methoxythiophene) (13.6 g, 59.4 mmol) in DMF, $POCl_3$ (13.0 g, 180.0 mmol) was added drop-wise at 0 ^oC, stirring was warmed neutralized by NaOH to neutrality. After extraction with $CHCl_3$, the organic phase was dried over $MgSO_4$. The crude product was purified by column chromatography on silica gel using ethyl acetate/petroleum ether (v/v = 1/4) as the eluent to give 9.49g pure product in 66.8 yield. Yellow oil; ^1H NMR (500 MHz, CDCl3) δ (ppm): 9.72 (s, 1H), 7.46 (s, 1H), 3.87 (s, 3H), 2.69 (d, 2H), 1.56-1.67(m, 1H), 1.21-1.37 (m, 8H), 0.84-0.92 (t, 6H).

5,15-Bis-(5-(2-ethylhexyl)-4-methoxythiophene)-2-yl)-porphyrin (S2):

A solution of 5-(2-(2-ethylhexyl)-3-methoxythiophene)-2-carbaldehyde (4.74g, 18.66 mmol) and dipyrromethane (2.72g, 18.66 mmol) in CH_2Cl_2 (1.5L) was purged with nitrogen for 30 min, and then trifluoroacetic acid (TFA) (0.22 mL) was added. The mixture was stirred for 12h at room temperature, and then 2,3-dichloro-5,6-dicyano-1,4-benzoquinone (DDQ) (6.90g) was added. After the mixture was stirred at room temperature for an additional 1h, the reaction was quenched by triethylamine (5 mL). Then the solvent was removed, and the residue was purified by flash column chromatography on silica gel using dichloromethane as the eluent. Recrystallization from CH_2Cl_2/methanol gave S**2** as a dark red solid (2.26g, 32%). ^1H NMR(500 MHz,

CDCl3) δ (ppm): 10.27 (s, 2H), 9.38 (s, 8H), 7.72 (s, 2H), 4.10 (s, 6H), 3.20 (d, 4H), 1.83-1.93(m, 2H), 1.40-1.69 (m, 16H), 0.97-1.17 (m, 12H), -2.97 (s, 2H).

5-bromo-10,20-bis[5-(2-ethylhexyl)-4-methoxythiophene-2-yl]-porphyrin (S3):

Porphyrin S**2** (1.26 g, 1.66mmol) were dissolved in 600 mL chloroform and pyridine (5 mL) and then cooled to 0 °C. To the cold solution, N-bromosuccinimide (295 mg, 1.66 mmol) was added and the mixture was stirred at 0 °C for 30 min. Then the reaction was quenched by acetone, and the mixture was washed with water and dried over anhydrous Na_2SO_4. After the solvent was removed, the residue was purified by flash column chromatography on silica gel using petroleum ether/dichloromethane (2:1) as the eluent. Recrystallization from CH_2Cl_2/methanol gave S**3** as a purple solid (0.90 g, 65%). ^{1}H NMR (500 MHz, $CDCl_3$) δ 10.11 (s, 1H), 9.73 (d, *J* = 4.8 Hz, 2H), 9.30-9.19 (m, 6H), 7.68 (s, 2H), 4.09 (s, 6H), 3.00 (dd, *J* = 7.0, 1.0 Hz, 4H), 1.92-1.78 (m, 2H), 1.68-1.37 (m, 6H), 1.04 (dt, *J* = 35.1, 7.2 Hz, 12H), -2.92 (s, 2H). ^{13}C NMR (126 MHz, $CDCl_3$) δ 153.1, 136.3, 132.6, 131.7, 125.5, 124.3, 112.9, 106.1, 104.4, 77.2, 59.4, 41.2, 32.8, 29.9, 29.1, 26.1, 23.2, 14.3, 11.1.

5-bromo-10,20-bis[5-(2-ethylhexyl)-4-methoxythiophene-2-yl]-porphinato)zinc (II) (S4):

Compound S**3** (904 mg, 1.08 mmol) was dissolved in a mixture of 200 ml chloroform. A solution of zinc acetate dihydrate (1.01 g, 5.4 mmol) in methanol (20 ml) was added, and the reaction mixture was stirred at 60 °C for 4 h. After routine

procedures, the solvent was evaporated, and the residue was chromatographed on silicagel using $CHCl_3$ as the eluent to give S**4** as a purple solid (953 mg, 98%).^{1}H NMR (500 MHz, $CDCl_3$) δ 9.97 (s, 1H), δ 9.84 (d, *J* = 4.6 Hz, 2H), 9.31 (d, *J* = 4.6 Hz, 2H), 9.26-9.18 (m, 4H), 7.52 (s, 2H), 3.90 (s, 6H), 2.87 (d, *J* = 6.9 Hz, 4H), 1.73-1.85 (m, 2H), 1.64-1.36 (m, 16H), 1.01 (dt, *J* = 23.4, 7.3 Hz, 12H). ^{13}C NMR (126 MHz, $CDCl_3$) δ 147.8, 147.7, 146.3, 145.8, 144.8, 132.6, 128.0, 127.6, 127.2, 126.4, 119.9, 119.01, 109.1, 104.5, 103.0, 54.6, 36.4, 28.0, 24.90, 24.3, 21.3, 18.4, 14.4, 9.5, 7.2, 6.3.

5-((Triisopropylsilyl)ethynyl)-10,20-bis[5-(2-ethylhexyl)-4-methoxythiophene-2yl]-porphinato)zinc (II) (S5):

The mono-bromo compound S**4** (920 mg, 1.02 mmol) was dissolved in THF (40 mL), and then triethylamine (20 mL) was added. The mixture was purged with argon for 30 min. Then $Pd(PPh_3)_2Cl_2$ (70 mg, 0.10 mmol), CuI (19 mg, 0.10 mmol), and (triisopropylsilyl)acetylene (926 mg, 5.1 mmol) were added. After the mixture was stirred at room temperature for 24 h under Ar, the reaction was quenched with brine. Then the mixture was extracted with dichloromethane, dried with anhydrous Na_2SO_4 and concentrated. Finally, the residue was purified on column chromatography to afford S**5** as a purple solid (940 mg, 92% yield). ^{1}H NMR (500 MHz, $CDCl_3$) δ9.98 (s, 1H), 9.84 (d, *J* = 4.6 Hz, 2H), 9.31 (d, *J* = 4.6 Hz, 2H), 9.26-9.18 (m, 4H), 7.52 (s, 2H), 3.90 (s, 6H), 2.87 (d, *J* = 6.9 Hz, 4H), 1.72-1.84 (m, 2H), 1.64-1.36 (m, 37H), 1.01 (dt, *J* = 23.4, 7.3 Hz, 12H). ^{13}C NMR (126 MHz, $CDCl_3$) δ 147.8, 147.7, 146.3,

145.8, 144.8, 132.6, 128.1, 127.6, 127.2, 126.4, 119.9, 119.1, 109.0, 104.5, 103.0, 96.5, 93.4, 54.6, 36.4, 28.0, 25.4, 24.9, 24.3, 21.3, 18.4, 14.4, 9.5, 7.2, 6.3.

5-bromo-15-((triisopropylsilyl)ethynyl)-10,20-bis[5-(2-ethylhexyl)-4-methoxythiophene-2yl]-porphinato)zinc (II) (S**6**):

Compound S**5** (900 mg, 0.89 mmol) was dissolved in 200 ml of chloroform and 2 ml of pyridine. After the reaction mixture was cooled to 0 ˚C, N-bromosuccinimide (240 mg, 1.35 mmol) was added to the reaction mixture and stirred for 30 min. Then the reaction mixture was washed with water, dried over Na_2SO_4, and concentrated. And the residue was purified first by column chromatography on silica gel to give S**6** as a dark green solid (689 mg, 71% yield). ^{1}H NMR (500 MHz, $CDCl_3$) δ 9.73 (d, *J* = 4.6 Hz, 2H), 9.62 (d, *J* = 4.6 Hz, 2H), 9.18 (d, *J* = 4.6 Hz, 2H), 9.14 (d, *J* = 4.7 Hz, 2H), 7.43 (s, 2H), 3.82 (s, 6H), 2.81 (d, *J* = 6.8 Hz, 4H), 1.79-1.68 (m, 2H), 1.61-1.35 (m, 37H), 1.00 (dt, *J* = 16.7, 7.3 Hz, 12H). ^{13}C NMR (126 MHz, $CDCl_3$) δ 153.3, 152.4, 151.5, 150.9, 149.5, 143.0, 137.2, 133.2, 133.0, 132.9, 131.4, 124.8, 123.9, 114.7, 109.2, 106.7, 101.4, 98.4, 77.2, 65.4, 59.3, 41.1, 32.7, 29.6, 29.0, 26.0, 23.2, 19.1, 19.0, 14.3, 11.9, 11.0.

4,7-Bis[(15-[(triisopropylsilyl)ethynyl]-10,20-bis[5-(2-ethylhexyl)-4-methoxythiophene-2yl]-porphinato)zinc(II)-5-ylethyny]benzo[*c*][1,2,5]thiadiazole (S7):

Compound **S6** (675mg, 0.62mmol) and 4,7-Diethynyl-benzo[*c*][1,2,5]thiadiazole

(50 mg, 0.27 mmol) were dissolved in THF (40 mL) with triethylamine (20 mL). Then Pd_2dba_3 (24 mg, 0.03 mmol) and $P(PPh_3)_4$ (72 mg, 0.06 mmol) were added. The mixture was stirred at 60 ^oC for 48 h under argon protection, then the reaction mixture was poured into water and extracted with $CHCl_3$ and washed with brine, dried over Na_2SO_4, and evaporated. The residue was chromatographed on silica gel to isolate the desired product, which was then further purified via GPC to afford compound S**7** (450mg, 76% yield). ^1H NMR (500 MHz, $CDCl_3$) δ 10.07 (d, *J* = 4.5 Hz, 4H), 9.67 (d, *J* = 4.5 Hz, 4H), 9.28 (d, *J* = 4.5 Hz, 4H), 9.16 (d, *J* = 4.4 Hz, 4H), 8.27 (s, 2H), 7.65 (s, 4H), 4.06 (s, 12H), 2.98 (d, *J* = 6.9 Hz, 8H), 1.89-1.78 (m, 4H), 1.68-1.35 (m, 74H), 1.02 (dt, *J* = 31.3, 7.3 Hz, 24H). ^{13}C NMR (126 MHz, $CDCl_3$) δ 155.4, 152.8, 152.5, 151.1, 150.9, 137.9, 132.9, 132.4, 131.4, 131.1, 124.4, 123.7, 117.6, 115.2, 109.8, 102.7, 102.4, 100.6, 98.11, 93.6, 77.3, 59.4, 41.2, 32.8, 29.8, 29.1, 26.1, 23.2, 19.1, 14.3, 11.9, 11.1.

4,7-Bis[(15-ethynyl-10,20-bis[5-(2-ethylhexyl)-4-methoxythiophene-2yl]-porphinato)zinc(II)-5-ylethyny]benzo[*c*][1,2,5]thiadiazole (1):

TBAF (1 M in THF, 0.46 mmol) was added to compound S**7** (436mg, 0.20 mmol) in 10 mL of THF at room temperature. After the mixture was stirred for 15 min, the mixture was poured into water, extracted with $CHCl_3$ and dried over Na_2SO_4, it was allowed to pass through a short silica gel column and to afford crude **8**, which were used directly for the next reaction without further purification.

ZnP2BT-RH: Compound **1** (187mg, 0.10 mmol) was dissolved in THF (20 mL) and triethylamine (10 mL) with compound **2** (0.30 mmol). Then $Pd(PPh_3)_4$ (12 mg, 0.01mmol) and CuI (2 mg, 0.01mmol) were added. After the mixture was stirred at 60 ^oC for 48 h under argon, the reaction was quenched with saturated brine. After the mixture was extracted with chloroform, dried with anhydrous Na_2SO_4 and concentrated. The residue was column chromatographed on silica gel using CH_2Cl_2 as eluent to give a black solid of **ZnP2BT-RH**. (170 mg, 65% yield).

ZnP2BT-RH: ^{1}HNMR (500 MHz, $CDCl_3$) δ/ppm (ppm): ^{1}HNMR (500 MHz, $CDCl_3$) δ/ppm (ppm): 10.66-9.60 (m, 16H), 8.58-7.73 (m, 12H), 7.58 (s, 4H), 6.45(s, 2H), 4.36 (s, 12H), 3.64-3.27 (m, 8H), 2.45-2.15 (m, 4H), 2.15-1.04 (m, 86H), 0.91 (s, 6H). MALDI−TOF Mass (m/z): calculated for $C_{142}H_{150}N_{12}O_6S_{11}Zn_2$: 2601.73; found: 2602.25; UV-vis (THF), λ_{max}=508 nm.

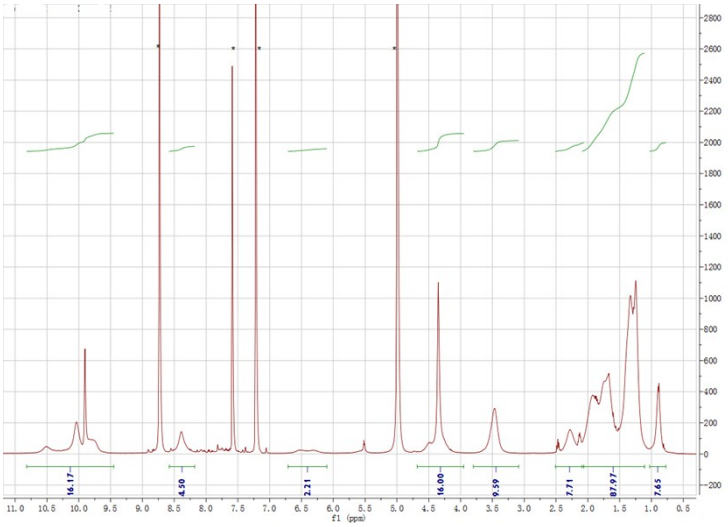

Figure S1. The ^{1}H NMR(500 MHz) spectrum of **ZnP2BT-RH** in Pyridine-d_5.

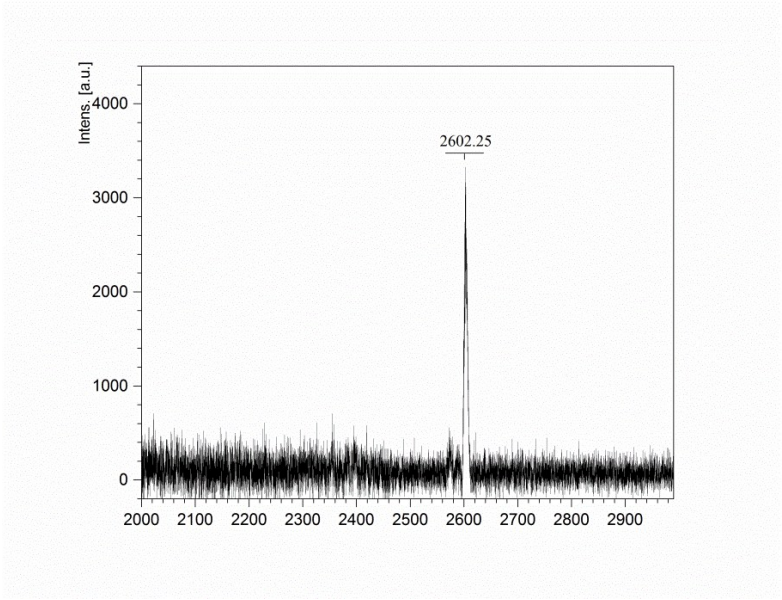

Figure S2. The high-resolution matrix-assisted laser desorption/ionization time-off light (MALDI-TOF) mass spectra of **ZnP2BT-RH**.

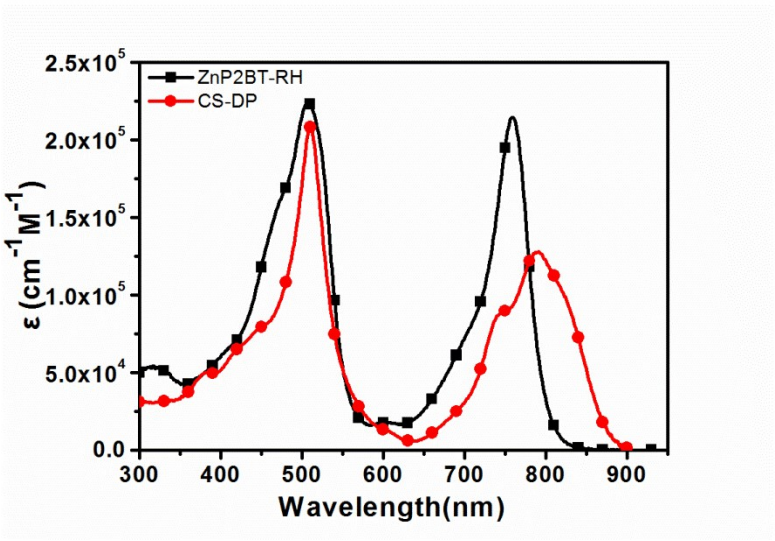

Figure S3. UV–vis–NIR absorption spectrum of ZnP2BT-RH and CS-DP in THF solution.

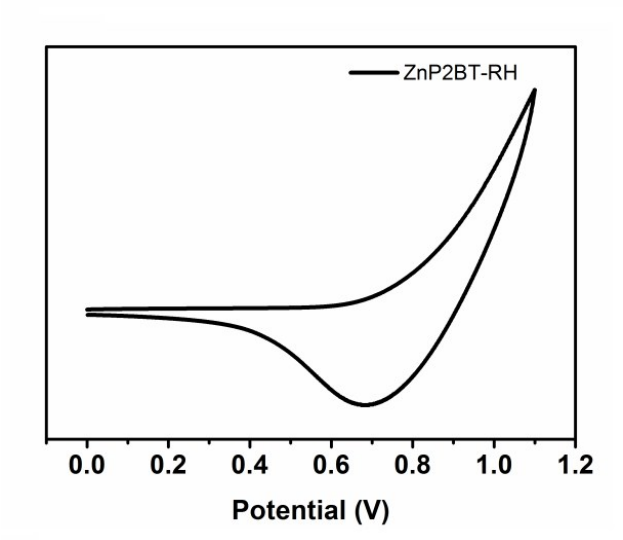

Figure S4. Cyclic voltammogram of ZnP2BT-RH film in acetonitrile containing 0.10 M tetrabutylammonium hexafluorophosphate (Bu_4NPF_6) as the supporting electrolyte and an Ag/AgCl electrode as the reference electrode speed of 50 mV s^{-1}.

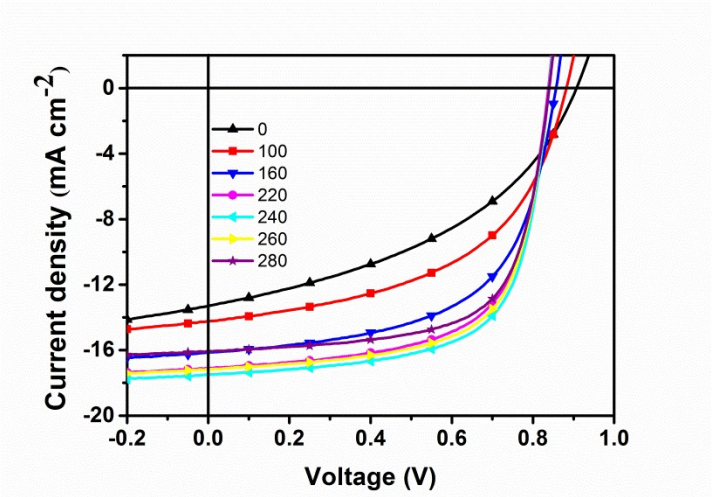

Figure S5. J-V curves of ZnP2BT-RH:$PC_{71}BM$ (w/w= 1:1.5) based solar cells under different SVA time.

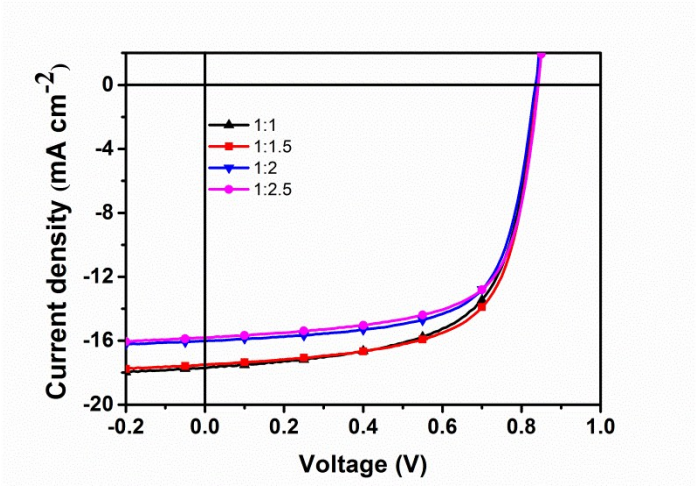

Figure S6. J-V curves of ZnP2BT-RH-based solar cells with various ZnP2BT-RH/$PC_{71}BM$ ratios under optimal SVA processing condition.

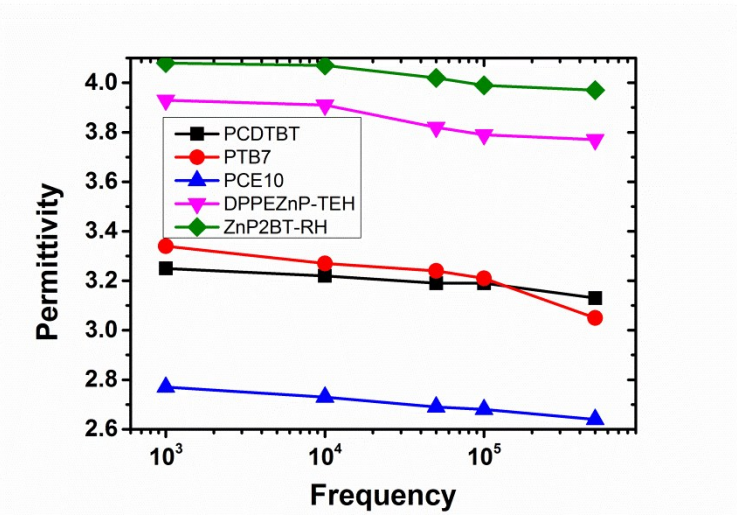

Figure S7. Relative dielectric constants (εr) of some small molecules and polymers with respect to frequency from 10^3 to 5×10^5 HZ.

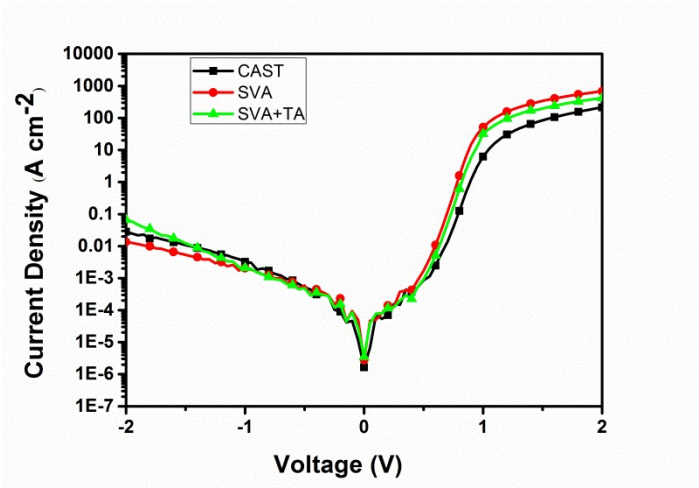

Figure S8. Dark J-V curves of ZnP2BT-RH-based solar cells under the different process conditions.

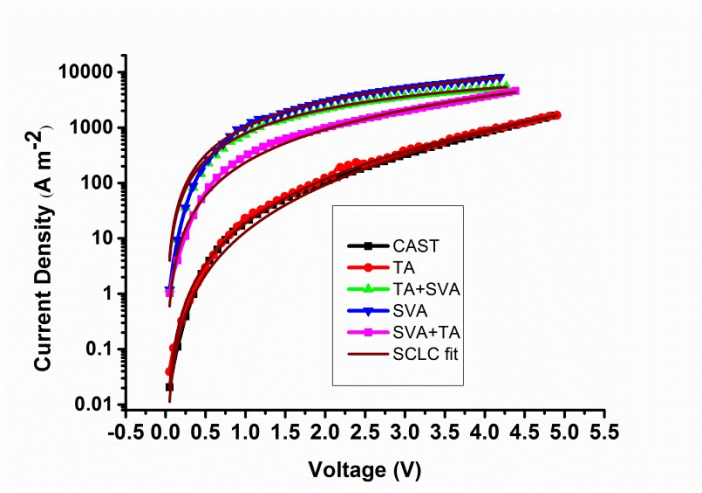

Figure S9. J-V characteristics in the dark under the different processing conditions based on device structures of ITO/PEDOT:PSS/ZnP2BT-RH:$PC_{71}BM$/MoO_3/Ag.

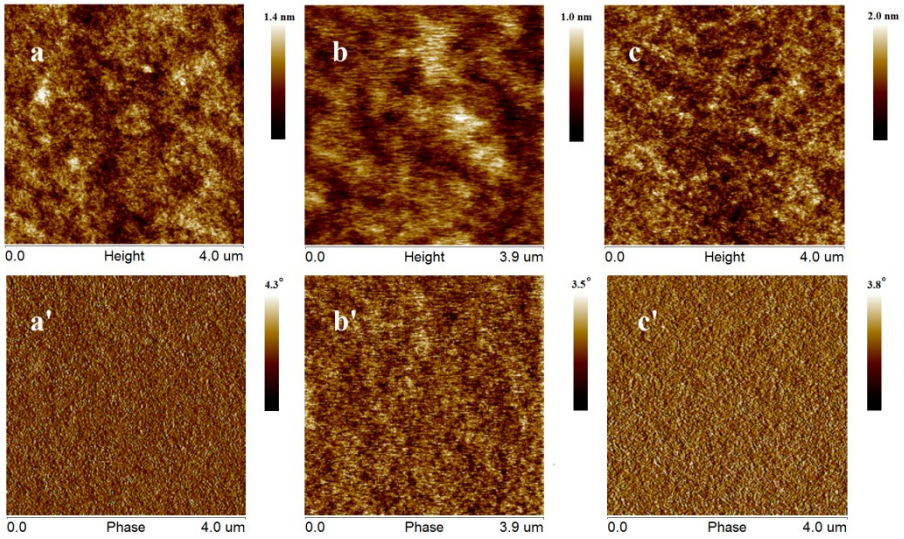

Figure S10. AFM height images (a-c) and phase images (a'-c') of ZnP2BT-RH:$PC_{71}BM$ blend films, a) as-cast, b) with SVA and c) TA+SVA.

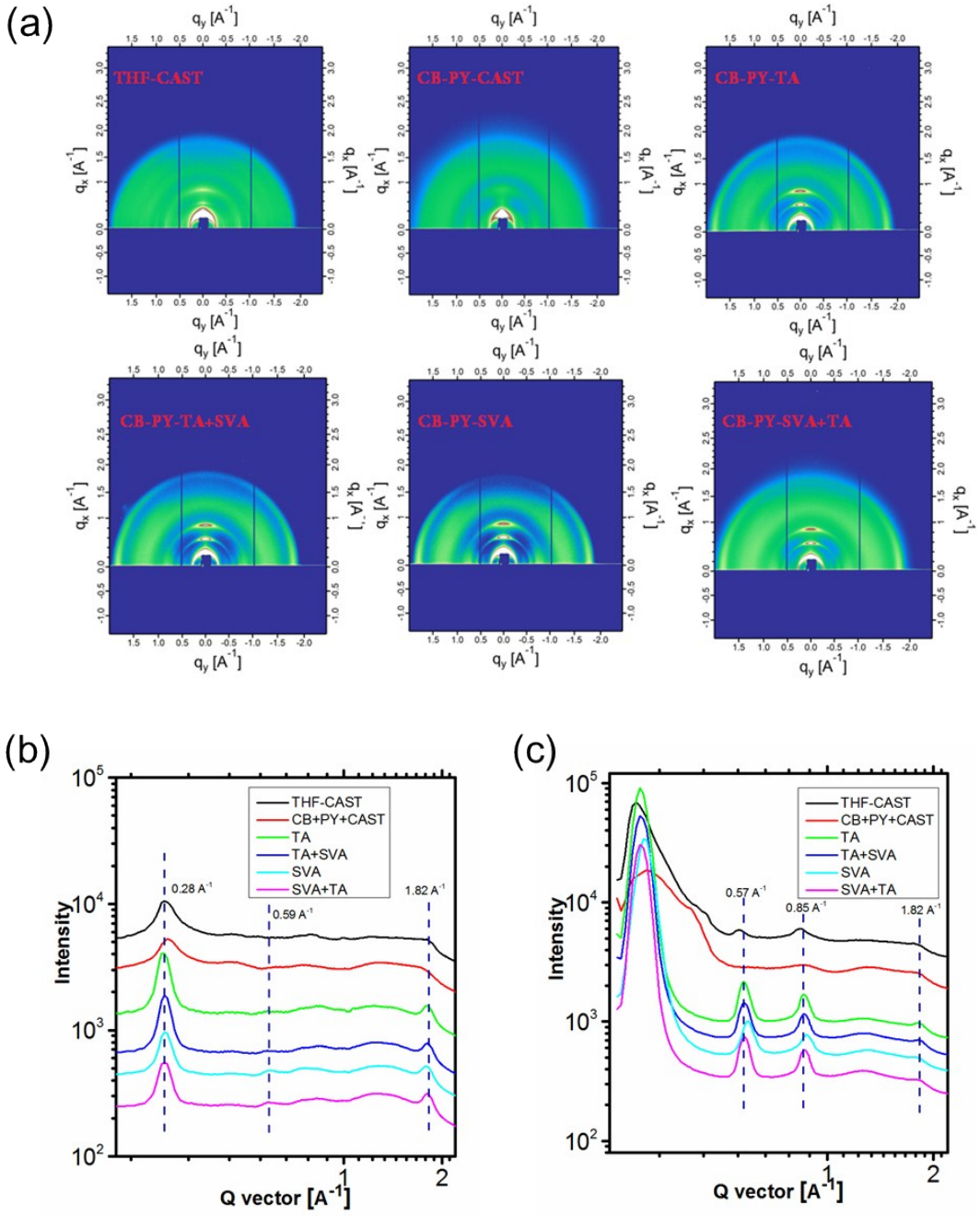

Figure S11. (a) Grazing incidence X-ray diffraction (GIXD) patterns, and (b) in-plane and (c) out-of- plane line-cut profiles of pure ZnP2BT-RH films.

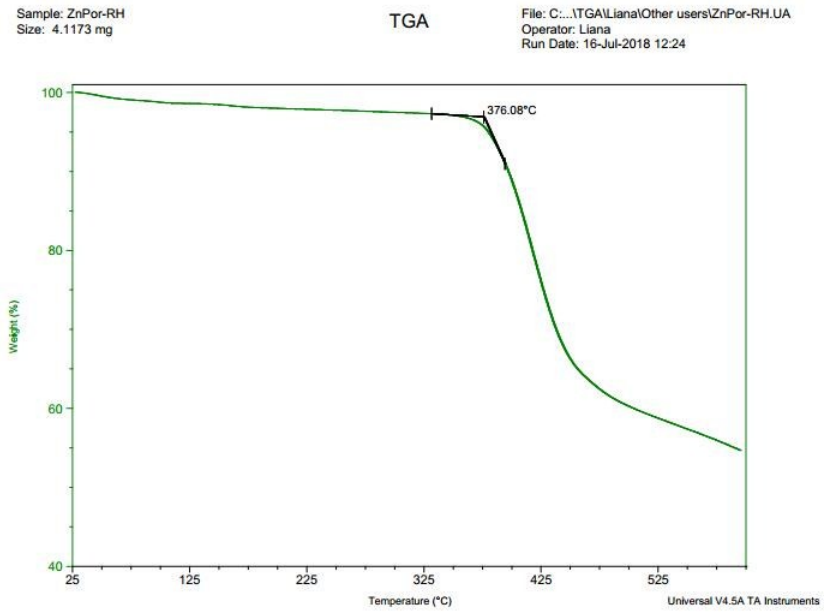

Figure S12. Thermogravimetric analysis results of ZnP2BT-RH

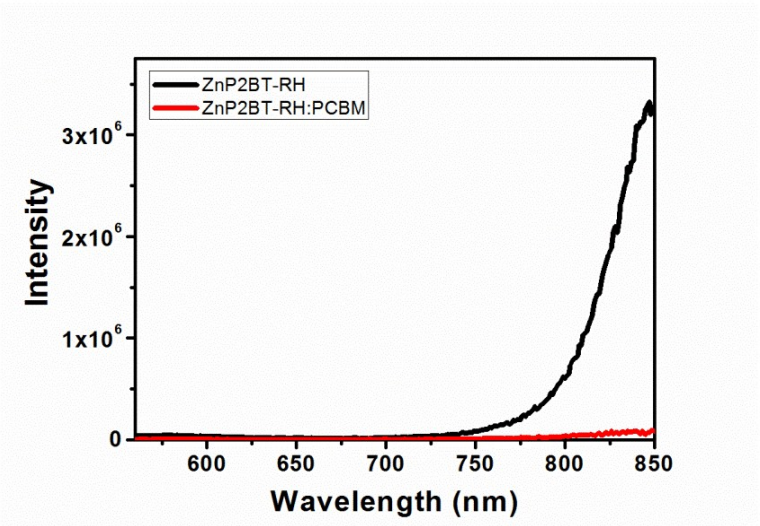

Figure S13. Photoluminescence spectra of ZnP2BT-PH film and its blend with $PC_{71}BM$ (Excitation wavelength: 535 nm).

Table S1. The photovoltaic parameters of ZnP2BT-RH:$PC_{71}BM$ (w/w= 1:1.5) based solar cells under different thermal annealing temperature.

temperature	J_{SC} (mA cm^{-2})	V_{OC} (V)	*FF* (%)	*PCE*(%)
RT	13.31±0.21	0.91±0.004	42.34±0.65	5.13±0.23(5.23)
120	13.78±0.22	0.91±0.005	42.32±0.55	5.31±0.19(5.23)
135	14.15±0.33	0.91±0.005	42.85±0.63	5.52±0.28(5.68)
150	13.45±0.32	0.90±0.005	40.75±0.53	4.93±0.20(5.05)

Table S2. The photovoltaic parameters of ZnP2BT-RH:$PC_{71}BM$ (w/w= 1:1.5) based solar cells under different SVA time.

SVA time (Seconds)	J_{SC} (mA cm^{-2})	V_{OC} (V)	*FF* (%)	*PCE*(%)
0	13.31±0.21	0.91±0.004	42.34±0.65	5.13±0.23(5.23)
100	14.22±0.22	0.88±0.004	51.72±0.55	6.48±0.21(6.67)
160	16.14±0.22	0.86±0.005	59.04±0.45	8.20±0.18(8.34)
220	17.08±0.23	0.84±0.005	64.89±0.56	9.31±0.25(9.51)
240	17.49±0.24	0.84±0.005	66.79±0.55	9.81±0.24(10.02)
260	17.16±0.24	0.84±0.005	66.45±0.49	9.58±0.23(9.70)
280	16.05±0.25	0.84±0.005	67.17±0.45	9.06±0.23(9.22)

Table S3. The photovoltaic parameters of ZnP2BT-RH-based solar cells with various ZnP2BT-RH:$PC_{71}BM$ ratio under optimal SVA processing condition.

weight ratio	J_{SC} (mA cm^{-2})	V_{OC} (V)	*FF* (%)	*PCE*(%)
1:1	17.82±0.24	0.84±0.005	63.53±0.55	9.51±0.18(9.61)
1:1.5	17.49±0.24	0.84±0.005	66.79±0.55	9.81±0.24(10.02)
1:2	16.02±0.22	0.84±0.005	67.81±0.44	9.12±0.19(9.24)
1:2.5	15.82±0.20	0.84±0.005	67.47±0.53	8.97±0.21(9.12)

Table S4. Summary of some high performance organic solar cells and with low energy loss.

Solar cells	PCEs	Material types		Bandgap (eV)	E_{loss} (eV)	Ref
		Molecules	Polymers			
DR3TSBDT:$PC_{71}BM$	9.95%	✓		1.74	0.83	4
BDTSTNTTR:$PC_{71}BM$	11.53%	✓		1.50	0.67	5
BIT6F:$PC_{71}BM$	9.09%	✓		1.79	0.90	6
BTID-2F:$PC_{71}BM$	11.30%	✓		1.68	0.73	7
PTB7-Th: F8IC	10.90%		✓	1.27	0.64	8
PNOz4T:$PC_{71}BM$	8.90%		✓	1.52	0.56	9
J61:ITIC	9.53%		✓	1.57	0.68	10
P3TEA:SF-PDI2	9.50%		✓	1.72	0.61	11
PffBX-T3:ITIC-Th	7.40%		✓	1.60	0.53	12
PBDTT-SF-TT: $PC_{71}BM$	9.07%		✓	1.59	0.59	13
PffBT4T-2DT:IDTBR	10.00%		✓	1.62	0.55	14
ZnP2BT-RH:PC71BM	10.02%	✓		1.40	0.56	This work

Table S5. Hole mobility of ZnP2BT-RH:$PC_{71}BM$ based devices.

conditions	As-Cast	TA	TA+SVA	SVA	SVA+TA
Value ($cm^2\ V^{-1}\ s^{-1}$)	1.21×10^{-5}	1.43×10^{-5}	3.40×10^{-4}	4.94×10^{-4}	1.08×10^{-4}

References

1. W. Huag, M. L. Li, L. Z. Zhang, T. B. Yang, Z. Zhang, H. Zeng, X. Zhang, L. Dang and Y. Y. Liang, *Chem Mater*, 2016, **28**, 5887-5895.
2. T. Lai, X. Chen, L. Xiao, L. Zhang, T. Liang, X. Peng and Y. Cao, *Chem Commun*, 2017, **53**, 5113-5116.
3. J. J. Bryant, B. D. Lindner and U. H. F. Bunz, *J Org Chem*, 2013, **78**, 1038-1044.
4. B. Kan, Q. Zhang, M. M. Li, X. J. Wan, W. Ni, G. K. Long, Y. C. Wang, X. Yang, H. R. Feng and Y. S. Chen, *J Am Chem Soc*, 2014, **136**, 15529-15532.
5. J. H. Wan, X. P. Xu, G. J. Zhang, Y. Li, K. Feng and Q. Peng, *Energ Environ Sci*, 2017, **10**, 1739-1745.
6. J. L. Wang, K. K. Liu, J. Yan, Z. Wu, F. Liu, F. Xiao, Z. F. Chang, H. B. Wu, Y. Cao and T. P. Russell, *J Am Chem Soc*, 2016, **138**, 7687-7697.
7. D. Deng, Y. J. Zhang, J. Q. Zhang, Z. Y. Wang, L. Y. Zhu, J. Fang, B. Z. Xia, Z. Wang, K. Lu, W. Ma and Z. X. Wei, *Nat Commun*, 2016, **7**, 13740-13748.
8. P. Cheng, M. Y. Zhang, T. K. Lau, Y. Wu, B. Y. Jia, J. Y. Wang, C. Q. Yan, M. Qin, X. H. Lu and X. W. Zhan, *Adv. Mater.*, 2017, **29**, 1605216-1605221.
9. B. Kan, Q. Zhang, M. M. Li, X. J. Wan, W. Ni, G. K. Long, Y. C. Wang, X. Yang, H. R. Feng and Y. S. Chen, *J. Am. Chem. Soc.*, 2014, **136**, 15529-15532.
10. K. Kawashima, Y. Tamai, H. Ohkita, I. Osaka and K. Takimiya, *Nat. Commun.*, 2015, **6**, 10085-10093.
11. H. J. Bin, Z. G. Zhang, L. Gao, S. S. Chen, L. Zhong, L. W. Xue, C. Yang and Y. F. Li, *J. Am. Chem. Soc.*, 2016, **138**, 4657-4664.
12. J. Liu, S. S. Chen, D. P. Qian, B. Gautam, G. F. Yang, J. B. Zhao, J. Bergqvist, F. L. Zhang, W. Ma, H. Ade, O. Inganas, K. Gundogdu, F. Gao and H. Yan, *Nat. Energy*, 2016, **1**, 16089-16095.
13. J. Zhang, K. Jiang, G. Yang, T. Ma, J. Liu, Z. Li, J. Y. L. Lai, W. Ma and H. Yan, *Adv. Energy Mater.*, 2017, DOI: 10.1002/aenm.201602119, 1602119-n/a.
14. Z. Du, X. Bao, Y. Li, D. Liu, J. Wang, C. Yang, R. Wimmer, L. W. Städe, R. Yang and D. Yu, *Adv. Energy Mater.*, DOI: 10.1002/aenm.201701471, 1701471-n/a.